SoftwareX 29 (2025) 102065

Contents lists available at ScienceDirect

SoftwareX

journal homepage: www.elsevier.com/locate/softx

Original software publication

microStabilize: In-plane microstructure stabilization in optical microscopy via normalized correlation coefficient matching method

Marek Grzegorz Mikulicz

Department of Experimental Physics, Faculty of Fundamental Problems of Technology, Wrocław University of Science and Technology, Wybrzeże Wyspiańskiego 27, Wrocław 50-370, Poland

ARTICLE INFO

Keywords:
Stabilization
OpenCV
Spectroscopy
Quantum dots

ABSTRACT

In this work, an automatic vision-guided accurate positioning of a microstructure in an optical microscope is presented. Microscopes for near-infrared spectroscopy are using actuators with micrometer and nanometer precision to investigate semiconductor nanostructures. The cryostats used to cool down the structures and other mechanical elements are an inevitable source of vibrations and sample drift in the optical setup. This is one of the challenges of long-term experiments in obtaining reliable data that require excitation and detection from the same spot on the sample. Consequently, the need for setup design and software that utilizes active stabilization of a sample position has emerged. Presented Python-based software with GUI utilizes the normalized correlation coefficient matching method from the openCV library to localize microstructure and automatically compensate for any misalignment with pixel accuracy and 0.2 μm precision in real-time.

Code metadata

Current code version	1.0
Permanent link to code/repository used for this code version	https://github.com/ElsevierSoftwareX/SOFTX-D-24-00363
Permanent link to Reproducible Capsule	–
Legal Code License	GNU General Public License v3.0
Code versioning system used	git
Software code languages, tools, and services used	Python
Compilation requirements, operating environments & dependencies	OpenCV, PySimpleGUI, imutils, NumPy, pygame
If available Link to developer documentation/manual	Developer guides available in the readme file in the GitHub repository
Support email for questions	marek.mikulicz@pwr.edu.pl

1. Introduction

1.1. Motivation and significance

Microphotoluminescence (μPL) is a standard tool for characterizing the properties of semiconductor nanostructures. This technique allows for the derivation of the electronic structure, the conduction and valence band structure, the dynamics of relaxation and recombination in nanometer-sized semiconductor structures such as quantum dots (QDs) with spatial confinement leading to quantization of energy levels [1]. This is achieved by measuring their optical response, where the composition, size, strain, shape, excitonic, and many-body effects affect both the energy and temporal statistics of the emitted photons. Experimentally, the optical characterization in a microscope typically involves excitation of a QD with a laser source with a focused spot spatial resolution on the order of micrometers. Emitted photons are guided and dispersed in the experimental setup where their energy, polarization, and temporal statistics are measured and contain information about the splitting between the energy bands, fine-structure splitting, single-photon emission statistics, photon indistinguishability, and excitonic complexes recombination dynamics.

In optical spectroscopy setups, numerous sources of vibrations and drift can lead to misalignment and inaccuracies in data collection. These sources include mechanical components such as cryostats, vacuum pumps, compressors, and air conditioning systems connected to or near the optical table. Additionally, piezoelectric elements used for fine adjustments of optical components, such as microscope objectives,

E-mail address: marek.mikulicz@pwr.edu.pl.

https://doi.org/10.1016/j.softx.2025.102065
Received 4 July 2024; Received in revised form 3 December 2024; Accepted 19 January 2025
Available online 31 January 2025

are prone to inherent factors such as hysteresis, creep, and thermal drift. The servo motors used to move the cryostat with a sample exhibit backlash and limited repeatability. Moreover, measurements conducted in large magnetic fields or those dependent on temperature variations of the sample can alter the excitation and detection spots. These disturbances are particularly problematic in long-term experiments, where consistent excitation and detection are required from the same spot on the sample.

In this work, the focus is on software and experimental setup for near-infrared spectroscopy used for the investigation of semiconductor QDs emitting at the third telecom window. To repeatedly investigate the same single QD and also to modify its properties, it is typically embedded in the photonic micro-structure such as a mesa [2] or microlens [3,4]. This microstructure can be fabricated as a cylinder embedding a single quantum dot of nanometer size. Typically, experimental measurements of the second order autocorrelation [5] (determining their single-photon purity) for signals from QDs in the third telecom window require several hours of data acquisition, during which the optical alignment must remain stable. Without active stabilization, the sample position is usually lost within a few minutes, causing the signal to disappear and requiring continuous manual adjustments, which is suboptimal for long experiments.

To stabilize the sample, various methods are used. One of the most precise are the laser interferometer position measurement systems with nm-precise positioning control, but they require costly additional hardware, which is more suited for more advanced systems such as electron-beam lithography [6], scanning electron microscopes [7], or atomic force microscopy [8]. This method is not easily available to custom-made optical setups with cryostats operating at the liquid helium temperature.

To provide an accurate, customizable, and low-cost solution, microStabilize has been developed, an open-source software with a graphical user interface that allows researchers to use already existing hardware (actuators and camera) in the optical setup and, without extensive modification to the setup, to achieve pixel-accurate long-term stabilization of the sample.

The software uses information from the microscope camera to continuously determine the position of the microstructure inside a cryostat. The cryostat is mounted on a stage with in-plane motorized steppers, and a microscope objective is mounted on a stage with piezo actuators. Stabilization is achieved by either moving the cryostat with a sample or an objective depending on the setup configuration (moving the objective introduces a slight misalignment in the detecting axis, which is not preferable). By continuously comparing a template image to the current frame in the microscope, detection and correction for any misalignment is possible by compensating it with actuator movement, ensuring that the sample remains correctly aligned throughout the data acquisition.

In the following discussion, the basic structure and architecture of microStabilize are detailed, and its software capabilities are highlighted. An illustrative example and performance evaluation are also provided.

1.2. Software contribution

The program has been tested and used internally in the laboratory for Optical Spectroscopy of Nanostructures (https://osn.pwr.edu.pl) by Ph.D. students and researchers, and was instrumental in enabling long-term measurements of the photon statistics [4,9–11]. In a publication investigating the excitonic and optical properties of single quantum dots [9] the results for autocorrelation measurements are presented for 15 quantum dots, accounting in total for at least 150 h of measurement for which active stabilization with the use of the microStabilize was maintained. The software can also be used in multiple excitation and detection configurations, for example, where the sample is placed perpendicularly and the signal collection is on a different axis from the excitation and image collection [10]. In investigating the microstructure in the bullseye cavity design, active stabilization was also used and allowed the measurement of autocorrelation for a few hours [11] measuring the single-photon emission of the QDs.

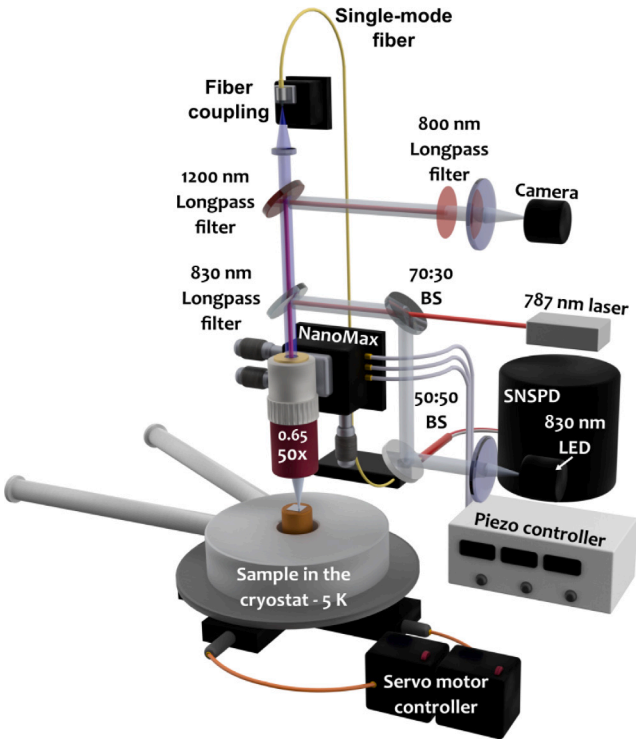

Fig. 1. Experimental setup used for the performance evaluation of the software.

1.3. Experimental setup

Data presented here are from a setup for near-infrared μPL shown in Fig. 1 which consists of an infinity corrected microscope objectives (magnifications from 10× to 100×, Mitutoyo, presented data are for M Plan Apo NIR HR 50× with NA of 0.65), tube lens (focal length 20 cm), LED microscopy illumination source (830 nm), monochrome camera (WAT-902B Watec), excitation laser (λ = 787 nm Coherent CUBE), spectral filter (fiber-based – WL Photonics or monochromator – Acton SP2500), signal detector (superconducting nanowire single photon detectors – Scontel or InGaAs – PyLoN-IR) all spectrally matched to the investigated spectral window (i.e. 1550 nm). The sample is mounted inside an evacuated continuous-flow liquid helium cryostat (ST-500 JANIS), which provides an operating temperature of about 5 K. The cryostat is mounted on an x–y stage with servo actuators. The calculations in the performance evaluation section were performed using a resolution test target (Thorlabs) placed in a sample position. The software was tested using two types of actuators; one of them is a 3-axis stage with an open-loop piezoelectric actuator from Thorlabs (NanoMax). These piezo actuators offer 20 µm of travel with a resolution of up to 1 nm. They are connected to the three-channel piezo controller with driving voltage up to 150 V. The control voltage can be modified by rotary knobs or by an external signal via USB 2.0 or BNC.

The other actuator is a Z925B servo motor actuator with a travel of 25 mm and a minimum incremental motion in the nanometer range. Its backlash and repeatability in the micrometer range make it less precise to use than a piezo actuator, but the large travel range allows it to cover a wide sample area. This actuator is driven by the controller (KDC101) via USB 2.0.

2. Software description

The microStabilize code is available to the public on GitHub, complete with documentation. Given that Python, NumPy [12] and OpenCV [13] libraries are open source and cross-platform (the software can run on Windows, Linux, and macOS), while LabView requires a paid license, Python was chosen, also because of its easier code customization compared to C++. Additionally, Python's clear syntax, vast libraries, and large user community make it an ideal choice for open-source projects. PySimpleGUI was chosen as the GUI framework because it prioritizes simplicity, rapid development, and ease of use for the user, which are crucial for the laboratory setting. Installation is straightforward and does not require specialized expertise. It can be easily implemented in standard spectroscopy laboratories, and the software can be integrated with the same hardware quickly and with customized hardware in a few hours.

2.1. Algorithms

2.1.1. Normalized correlation coefficient matching

The core functionality of the program is based on the normalized correlation coefficient matching method from the openCV library. During development, all template matching algorithms in the library were tested, as well as the phase correlation approach [14] and the Haar cascade classifier. The correlation coefficient matching method provides the most precise and distinct match; however, it increases the computational cost that limits the frame size depending on computer resources. It is more versatile than neural network-based models, as there is no need to provide training examples and only one template snapshot is required for tracking. The algorithm works for differences in translation, brightness, and contrast, which are typically present in an optical microscopy setup. The algorithm adjusts the template and image to have a zero mean by transforming the dark parts of the image into negative values and the bright parts into positive values. This adjustment ensures that when bright regions of the template overlap with bright regions of the image, the resulting dot product is positive. Similarly, when dark regions overlap, the product of two negative values also results in a positive score. Therefore, positive scores indicate matches between the corresponding bright and dark regions of the template and image. In contrast, mismatches, such as a dark region in the template overlapping with a bright region in the image, result in negative values. The calculations are as follows:

$$R(x,y) = \frac{\sum_{x',y'} \left(T'(x',y') \cdot I'(x+x',y+y')\right)}{\sqrt{\sum_{x',y'} T'(x',y')^2 \cdot \sum_{x',y'} I'(x+x',y+y')^2}} \tag{1}$$

$$T'(x',y') = T(x',y') - \frac{1}{(w \cdot h)} \cdot \sum_{x'',y''} T(x'',y'') \tag{2}$$

$$I'(x+x',y+y') = I(x+x',y+y') - \frac{1}{(w \cdot h)} \cdot \sum_{x'',y''} I(x+x'',y+y'') \tag{3}$$

where: I is the source image, T is the patch image that is compared to the source image, w and h are equal to the width and height of the template image, respectively. The $x' = 0 \cdots w-1$, and the $y' = 0 \cdots h-1$. The template is moved one pixel at a time (left–right, up-down). And for every location, a metric R is calculated that returns values between -1 and 1 indicating the degree of correlation between T and I at a given position, forming a result matrix R where in the software the function minMaxLoc() is used to return the highest value in the R matrix. In the program, this newfound location (X', Y') is compared in every frame with the old location (X, Y) set when the user was selecting the region of interest (ROI). The difference between these locations $(X-X', Y-Y')$ is calculated and returned $(\Delta X, \Delta Y)$. If the set pixel threshold value (for highest accuracy, typically set to 0) is exceeded, the program moves the motors until the difference is not higher than the threshold (typically when $\Delta X = 0$ and $\Delta Y = 0$), which causes ROI to return to its origin position.

2.1.2. Focus detection

The focus value for the frame is determined by calculating the variance of the Laplacian of the frame. The Laplacian of an image represents a two-dimensional isotropic measure of the second spatial derivative of an image. This Laplacian emphasizes areas of quick change in brightness, which for moving the microscope objective in the z direction, allows finding the position with the highest image contrast — the in-focus position. For an image, the Laplacian can be calculated using a convolution filter with a frame with a small kernel:

$$\begin{bmatrix} 0 & -1 & 0 \\ -1 & 4 & -1 \\ 0 & -1 & 0 \end{bmatrix} \quad \text{and} \quad \begin{bmatrix} -1 & -1 & -1 \\ -1 & 8 & -1 \\ -1 & -1 & -1 \end{bmatrix}$$

2.2. Software architecture

Fig. 2 illustrates the workflow of the image processing and motor control system, which integrates three levels: GUI and frame, Software, and OpenCV library. At the GUI Level (blue), the user initiates the process, initializes actuators and joystick, selects the Region of Interest (ROI), stabilizes the ROI, exits the application, the frame size can be changed and its brightness and contrast can be modified, and the user can add an indicator of a laser spot. The Software Level (green) handles initialization, frame reading, ROI management, actuator movements, and joystick inputs in various directions. It captures image frames, calculates FPS, processes user inputs, and adjusts motor positions as needed. The OpenCV Library Level (red) performs key image processing tasks. It uses the Laplace operator to calculate the focus value and normalized correlation coefficient matching to track the ROI position on the window.

2.3. Software functionalities

The main purpose of the software is to track and automatically stabilize with high precision the sample in the μPL setup. The following are the key features and functionalities:

- Sample stabilization — after selecting the ROI and initializing the actuators by the user, the selected ROI is compared to the frame, and the difference to the ROI origin position is calculated. With stabilization active, the actuators are moved to minimize the calculated difference. This movement is continuously adjusted to ensure the ROI remains at the origin position, effectively stabilizing the sample. The software utilizes the normalized correlation coefficient matching method to determine the x and y shifts required for alignment. Throughout the stabilization process, the software continuously monitors frame metrics such as confidence and difference values, and the user can observe real-time feedback on the frame window.
- Sample position control — in software there is implemented a connection with the joystick controller which enables users movement in x, y, and z axes. The software allows users to adjust the speed of the movement and also for small incremental steps to the sample's position, which is particularly useful for high-magnification setups.
- Remote control — combination of displaying of the frame window and position control in one software enables easy remote control of the experimental setup. Isolation of the experimental setup minimizes physical disturbances and optical noise.
- Extensive GUI — intuitive user interface lowers the barrier for the users with less experience to start experiments. The GUI allows user to change brightness and contrast of the frame from the optical microscope. The functionality to add laser spot at the desired position allows user to track the position of the laser even if it is filtered before the imaging camera — this functionality commonly used in μPL experiments where user do not want laser to obstruct the view of the structure but to know its position.

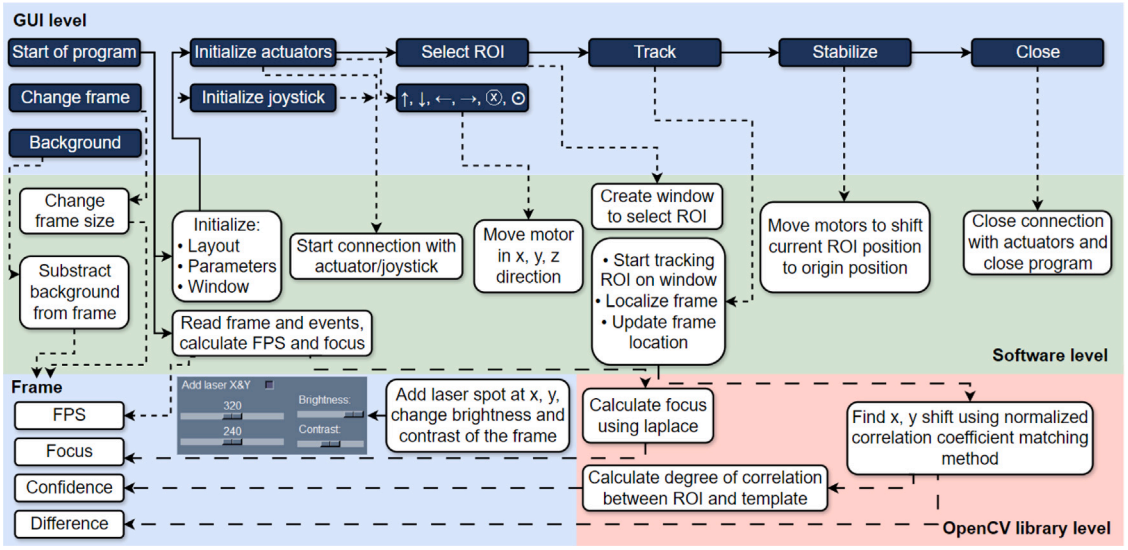

Fig. 2. The flowchart demonstrates the integration between GUI, software, and OpenCV library levels. Solid arrows show the standard order of operations in the workflow.

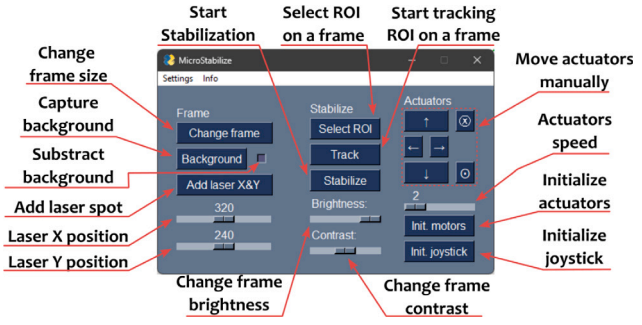

Fig. 3. Graphical user interface for controlling the software, modifying the frame, setting up stabilization and controlling actuators.

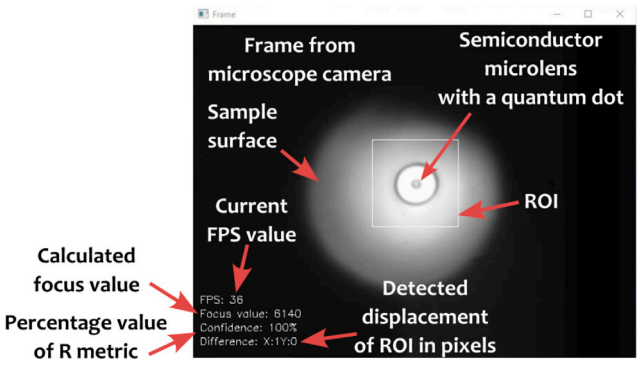

Fig. 4. Real-time microscope view display of a semiconductor microlens with a quantum dot using a microscope camera. The displayed frame includes key metrics: current frames per second (FPS), calculated focus value, confidence percentage of the R metric, and detected displacement of the region of interest (ROI). These metrics aid in assessing the stability and focus of the sample during long-term experiments. The ROI highlights the tracked area.

- Finding template — user can load an image in which loaded template will be localized and its coordinates will be printed in console along with confidence level.
- Background subtraction — in low light sample illumination conditions the background subtraction enables user to increase the visibility of the investigated structure.
- Focus detection — by creating a metric for the focus value, this functionality helps users track and return to the same experimental conditions.

3. Illustrative examples

In Fig. 3 the graphical user interface of the program is presented with every element described. This interface is divided into three sections: Frame, Stabilize, and Actuators, each responsible for controlling respective functionality. The second window of the software is the frame from the camera visible in Fig. 4 displaying the view from the microscope. It allows the user to see the current FPS, the focus value, the percentage value of the R metric, and the difference between the current ROI position and its origin position. These two windows are separated to allow the user to split them between the monitors in the laboratory for easier operation. After starting the software, the typical workflow is as follows: the user initializes the motors and joystick, moves the actuators to localize the structure, selects ROI, starts tracking, and stabilizing.

4. Performance evaluation

Performance of the detection algorithm was evaluated with the microlens [4] shown in Fig. 4 with a 50× microscope objective and a motorized actuator as shown in the experimental setup section. After selecting the ROI, its position was tracked without stabilization as shown in Fig. 5, and a 6.5 μm drift of the microstructure was observed during 6 min, the setup vibrations are also visible. After starting the stabilization, the sample returned to its origin position in 20 s. Long-term tracking with and without stabilization of the position of the sample on the x and y axes is shown in Fig. 6 showing a large drift of up to 6 μm in one axis. With stabilization on, the accuracy, taken as the mean position, is below the single pixel level, and the precision, taken as the standard deviation, is below 1.5 px. In practice, this precision is enough for stable operation for long-term experiments without loss of signal intensity.

To evaluate the robustness of the software to the data with decreasing quality, 40 images with increasing Gaussian blur [15] were generated. This represents a situation when the microscope objective (or a lens) is slightly de-focused, which can happen in the experimental setup. A result of the correlation coefficient value in template matching as a function of blur radius is shown in Fig. 7; it was fitted with a

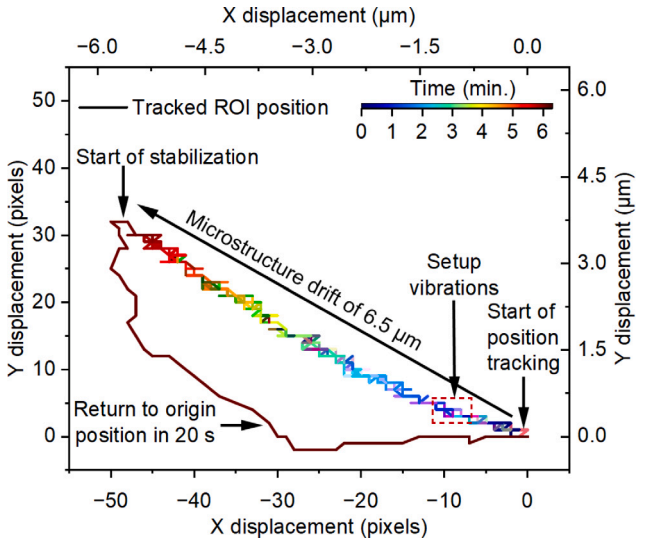

Fig. 5. 2D trajectory of the ROI displacement before and during the active stabilization. The figure illustrates a microstructure drift of 6.5 µm in 6 min. Active stabilization achieves a pixel-accurate return to origin position with stabilization speed of 0.3 µm/s. Without active stabilization the microstructure vibrations within a few pixels range are also visible.

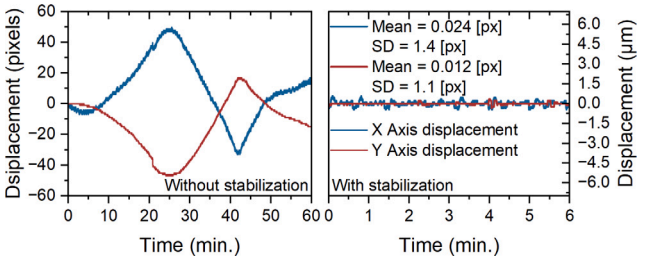

Fig. 6. Comparison of displacement over time with and without stabilization. a) Displacement of the X and Y axes in pixels and micrometers over 60 min without stabilization. Significant drift is observed in both axes. (b) Displacement of the X and Y axes in pixels and micrometers over 6 min with stabilization. The mean displacements in both axes are close to zero and standard deviation in pixel range translates to precision of 0.2 nm which effectively reduces drift in both axes.

Gaussian function ($\sigma = 12$). In the software, the threshold for the R value is set to 0.70, if the correlation coefficient drops below that level, the software stops tracking.

5. Conclusions and impact

MicroStabilize, an open-source vision-guided software, has been developed to stabilize microstructures in near-infrared optical microscopes. This software utilizes micro- and nano-actuators to achieve fast operation and pixel-level accuracy. To use the software with the described hardware, no programming knowledge is required. Modifying a program can be done easily, and the system can be versatilely deployed using arbitrary actuators and optical imaging. This software overcomes limitations in terms of drift and vibrations in optical setups, especially for long-lasting μPL experiments. Existing commercial mechanical and piezoelectric micro- and nano-actuators are mainly operated manually despite having some semiautomatic features for programmed or stored positions, and this software offers easier operation and the possibility of remote control of an experimental setup. The prospective extension of this work is to perform pixel-accurate 2D μPL mapping of the structure, and with the z actuator, it is possible to create 3D photoluminescence tomography images, for example, to visualize the kinetics of charge carrier recombination [16]. The software facilitates

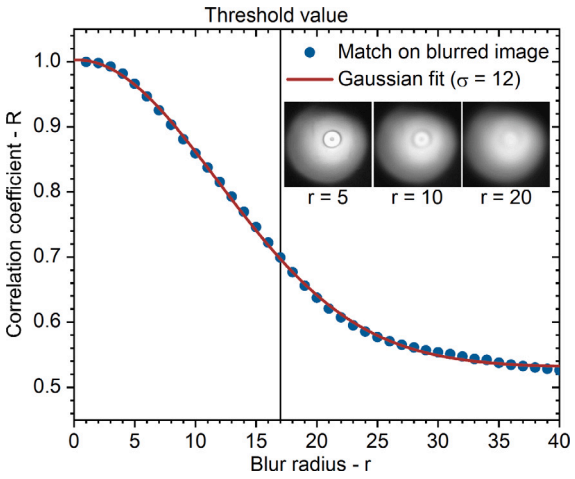

Fig. 7. Confidence of matched template as a function of blur radius. 1.0 (100% confidence) indicates a perfect match. The threshold value is a point where a matched template starts to shift by at least 1 pixel indicating decline in accuracy. Three images with an increasing level of blur are added to the graph.

the investigation of single-photon purity as a function of excitation power and temperature, quasi-resonant excitation photoluminescence scans, investigation of resonance fluorescence, and increased resolution of polarization-resolved measurements of fine-structure splitting. Precise localization also allows prospectively to perform vision-guided autonomous sequential localization and characterization of a large number of devices.

Declaration of competing interest

The author declares having no known competing financial interests or personal relationships that could have appeared to influence the work reported in this paper.

Acknowledgments

This work was funded by the National Science Centre (Poland) under Project No. 2020/39/D/ST5/02952, and partially funded by the European Union's Horizon Europe Research and Innovation Programme under the QPIC 1550 project (Grant Agreement No 101135785).

References

[1] Bockelmann U, Heller W, Filoramo A, Roussignol P. Microphotoluminescence studies of single quantum dots. I. Time-resolved experiments. Phys Rev B 1997;55(7):4456–68. http://dx.doi.org/10.1103/physrevb.55.4456.

[2] Marzin JY, Gérard JM, Izraël A, Barrier D, Bastard G. Photoluminescence of single InAs quantum dots obtained by self-organized growth on GaAs. Phys Rev Lett 1994;73(5):716–9. http://dx.doi.org/10.1103/physrevlett.73.716.

[3] Gschrey M, Thoma A, Schnauber P, Seifried M, Schmidt R, Wohlfeil B, et al. Highly indistinguishable photons from deterministic quantum-dot microlenses utilizing three-dimensional in situ electron-beam lithography. Nat Commun 2015;6(1). http://dx.doi.org/10.1038/ncomms8662.

[4] Jaworski M, Mrowiński P, Mikulicz MG, Holewa P, Zeidler L, Syperek M, et al. Xenon plasma-focused ion beam milling for fabrication of high-purity, bright single-photon sources operating in the C-band. Opt Express 2024;32(23):41089. http://dx.doi.org/10.1364/oe.534313.

[5] Pelton M, Santori C, Vučković J, Zhang B, Solomon GS, Plant J, et al. Efficient source of single photons: A single quantum dot in a micropost microcavity. Phys Rev Lett 2002;89:233602. http://dx.doi.org/10.1103/PhysRevLett.89.233602, URL: https://link.aps.org/doi/10.1103/PhysRevLett.89.233602.

[6] Pease RFW. Electron beam lithography. Contemp Phys 1981;22(3):265–90. http://dx.doi.org/10.1080/00107518108231531.

[7] Hatsuzawa T, Toyoda K, Tanimura Y. A metrological electron microscope system for microfeatures of very large scale integrated circuits. Rev Sci Instrum 1990;61(3):975–9. http://dx.doi.org/10.1063/1.1141202.

[8] Ducourtieux S, Poyet B. Development of a metrological atomic force microscope with minimized Abbe error and differential interferometer-based real-time position control. Meas Sci Technol 2011;22(9):094010. http://dx.doi.org/10.1088/0957-0233/22/9/094010.

[9] Wyborski P, Gawełczyk M, Podemski P, Wroński PA, Pawlyta M, Gorantla S, et al. Impact of MBE-grown (In,Ga)As/GaAs metamorphic buffers on excitonic and optical properties of single quantum dots with single-photon emission tuned to the telecom range. Phys Rev Appl 2023;20(4). http://dx.doi.org/10.1103/physrevapplied.20.044009.

[10] Burakowski M, Holewa P, Mrowiński P, Sakanas A, Musiał A, Sęk G, et al. Heterogeneous integration of single InAs/InP quantum dots with the SOI chip using direct bonding. Opt Express 2024;32(7):10874. http://dx.doi.org/10.1364/oe.515223.

[11] Holewa P, Vajner DA, Zięba-Ostój E, Wasiluk M, Gaál B, Sakanas A, et al. High-throughput quantum photonic devices emitting indistinguishable photons in the telecom C-band. Nat Commun 2024;15(1). http://dx.doi.org/10.1038/s41467-024-47551-7.

[12] van der Walt S, Colbert SC, Varoquaux G. The NumPy array: A structure for efficient numerical computation. Comput Sci Eng 2011;13(2):22–30. http://dx.doi.org/10.1109/mcse.2011.37.

[13] Bradski G. The OpenCV library. Dr Dobb's J Softw Tools 2000;25:120–5, URL: https://cir.nii.ac.jp/crid/1570009750919616256.

[14] Foroosh H, Zerubia J, Berthod M. Extension of phase correlation to subpixel registration. IEEE Trans Image Process 2002;11(3):188–200. http://dx.doi.org/10.1109/83.988953.

[15] Gwosdek P, Grewenig S, Bruhn A, Weickert J. Theoretical foundations of Gaussian convolution by extended box filtering. In: Scale space and variational methods in computer vision. Springer Berlin Heidelberg; 2012, p. 447–58. http://dx.doi.org/10.1007/978-3-642-24785-9_38.

[16] Stavrakas C, Zhumekenov AA, Brenes R, Abdi-Jalebi M, Bulović V, Bakr OM, et al. Probing buried recombination pathways in perovskite structures using 3D photoluminescence tomography. Energy Environ Sci 2018;11(10):2846–52. http://dx.doi.org/10.1039/c8ee00928g.